RESEARCH ARTICLE | MAY 16 2022

Single charge transport in a fully superconducting SQUISET locally tuned by self-inductance effects

Special Collection: 2022 Nanoscience and Nanotechnology

E. Enrico ; L. Croin; E. Strambini; F. Giazotto

AIP Advances 12, 055122 (2022)
https://doi.org/10.1063/5.0084168

Single charge transport in a fully superconducting SQUISET locally tuned by self-inductance effects

Cite as: AIP Advances 12, 055122 (2022); doi: 10.1063/5.0084168
Submitted: 19 April 2022 • Accepted: 3 May 2022 •
Published Online: 16 May 2022

E. Enrico,[1,a)] L. Croin,[1] E. Strambini,[2] and F. Giazotto[2]

AFFILIATIONS

[1] INRIM, Istituto Nazionale di Ricerca Metrologica, Strada delle Cacce 91, I-10135 Torino, Italy
[2] NEST, Istituto Nanoscienze-CNR and Scuola Normale Superiore, Piazza S. Silvestro 12, Pisa I-56127, Italy

[a)] **Author to whom correspondence should be addressed:** e.enrico@inrim.it

ABSTRACT

We present a single-electron device for the manipulation of charge states via quantum interference in nanostructured electrodes. Via self-inductance effects, we induce two independent magnetic fluxes in the electrodes and we demonstrate sensitivity to single charge states and magnetic field at variable temperature. Moreover, our approach allows us to demonstrate local and independent control of the single-particle conductance between nano-engineered tunnel junctions in a fully superconducting quantum interference single-electron transistor, thereby increasing the flexibility of our single-electron transistors. Our devices show a robust modulation of the current-to-flux transfer function via control currents while exploiting the single-electron filling of a mesoscopic superconducting island. Further applications of the device concept to single charge manipulation and magnetic-flux sensing are also discussed.

Superconducting nanoelectronics has continuously grown in the last few decades as a flexible and promising platform for the implementation of quantum-based sensors[1–3] and quantum-state manipulating circuits,[4,5] with particular attention to interference based superconducting devices[6] and mesoscopic structures where single charges play dominant roles.[7,8] Different geometries can be easily combined with standard nanolithography techniques,[9] opening the field to complex and robust devices embedding multiple control lines and tunable working points in the parameter space. As a consequence, superconducting nanoelectronics technology represents an exceptional research platform for condensed-matter quantum physics experiments as well as for scalable quantum computing[10] and photonics applications.[11]

Normal-metal,[12] hybrid,[13] or fully superconducting[14] single-electron devices—fabricated by the shadow-mask technique[9]—have been so far one of the research topics where nanofabrication technology excelled, leading to device concepts where the detection of charge states approaching their coherent superposition[15] has been routinely reached. While rather complex single-electron systems based on local electrical gating have been demonstrated,[16] the on-chip tunability of their electrodes' carrier population has been limited to the semiconductor nanowires[17] and the 2D-electron-gas based technologies,[18] where clear manipulation of Coulomb blockade effects has only been allowed via strong electric fields.

Nano-engineered superconducting electrodes[8] introduce an alternative control parameter, the magnetic flux, that can act on the population of quasiparticle charge carriers[19] via quantum interference.[1] Short metallic nanowires have been embedded in superconducting loops[7] leaving enough space to be coupled to a Coulombic island through mesoscopic tunnel junctions. The present technology, which is mostly based on aluminum tunnel junctions, is then further extended by an unprecedented level of control and flexibility offered by localized magnetic fluxes. Various approaches exploiting these phenomena demonstrated state-of-the-art magnetic flux sensing capabilities[2,3,20] and single charge state manipulation[8] but still lack for on-chip control.

Here, we demonstrate that two local magnetic fluxes can be used to manipulate the electrode density of states of a fully superconducting quantum interference single-electron transistor (SQUISET) and to efficiently modify its electron transport properties. In particular, we show how the typical Coulomb energy of the island can be controlled by the quasiparticle spectra of the source and drain electrodes by exploiting self-inductance effects.

A prototypical device is depicted in Fig. 1. A superconducting island is connected to the source and drain electrodes via tunnel junctions. Both source and drain consist of a superconducting nanowire embedded in a superconducting loop. Each ring has two contact pads for the injection of the source–drain current and the currents for the independent control of the fluxes. The entire structure is realized via three-angle-deposition ($42^\circ/20^\circ/0^\circ$) of aluminum (15/20/100 nm) through a suspended mask on a Si/SiO_2 (300 nm thick oxide) substrate [see Fig. 1(a)]. The polymeric mask has been obtained via electron beam lithography, whereas thin film deposition has been performed via electron beam evaporation. Tunnel junctions were created between the first and the second deposition step by oxygen exposure (5×10^{-2} mbar for 5 min). One of the tunnel junctions across the nanowire and the island is visible in the inset of Fig. 1(a). The device configuration defines three main current paths I_S, I_D, and I_{SD}. The first two act as control currents flowing along parts of the source and drain loops, while the last is the effective current flowing through the Coulombic island [Fig. 1(b)]. The entire chip is pierced by a uniform magnetic field, B, generated by an external magnet inducing a flux $\Phi_B = A * B$ in both the identical loops of area A. The combined effect of B and the local currents gives rise to two magnetic fluxes at the source and drain loops, $\Phi_S = \Phi_B + M_S * I_S + m_S * I_D$ and $\Phi_D = \Phi_B + M_D * I_S + m_D * I_D$, respectively. M_S and M_D are the self-inductances, while m_S and m_D are the mutual inductances between opposite loops. The electrodes are biased via an external voltage source (V_{SD}), and the island is exposed to a control electric field via a capacitively coupled gate that induces $n_G = C_G V_G/e$ quantized charges, with C_G being the gate–island capacitance, V_G the gate voltage, and e the electron charge. This device architecture is designed to act essentially as a fully superconducting single-electron transistor[21,22] with two identical tunnel junctions (total series resistance $R_T \approx 1.75$ MΩ). In the absence of a magnetic field, this is confirmed by the differential conductance stability diagram in Fig. 1(c) clearly showing the effect of the charging energy, evaluated to be $E_C = 75$ μeV from the Coulomb diamonds and confirmed by the Josephson-quasiparticle

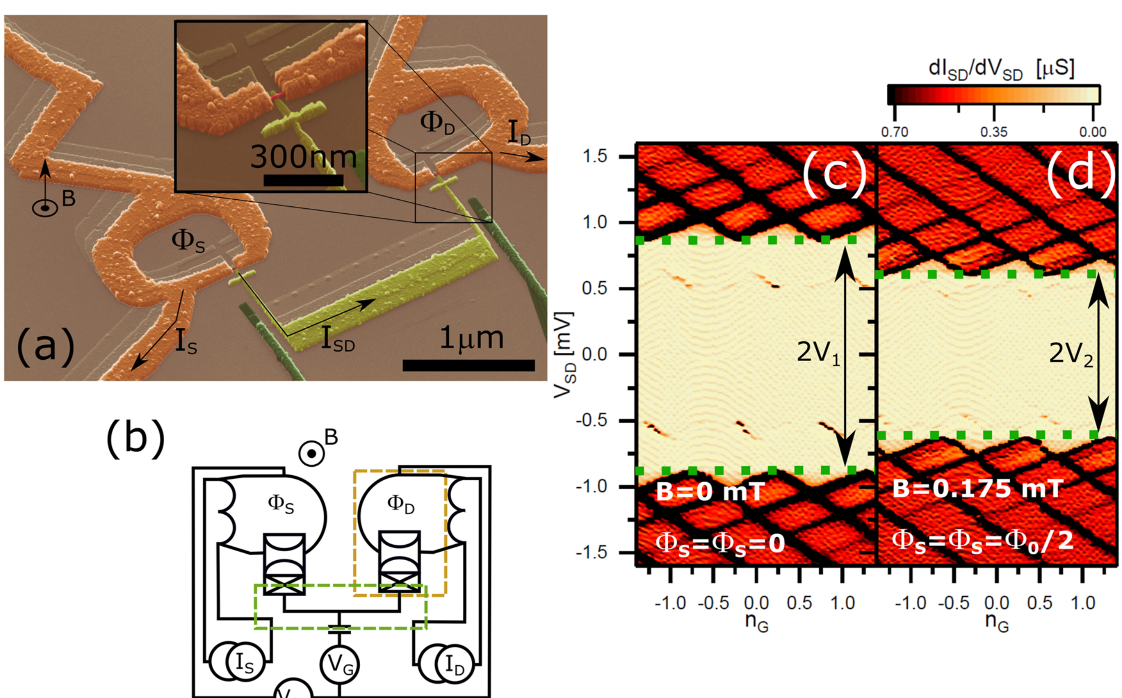

FIG. 1. (a) Scanning electron micrography of a typical SQUISET device. The two current paths (I_S and I_D) generating the two magnetic fluxes (Φ_S and Φ_D) are indicated. The latter pierce the two superconducting loops of the source and drain electrodes (orange). A mesoscopic island (light green) is in tunnel contact with two superconducting nanowires (red), and it is capacitively coupled to a gate electrode (green). Few elements of the device can be attributed to fabrication or measurement details. In particular, the cross-like structure reported by the inset near the nanowire is its unavoidable duplicate coming from the shadow deposition technique used to fabricate the structure. Always in the shadow technique context, the fork-like structure of the gate electrodes guarantees a fixed distance between the island and the gate at every deposition angle. The structure with sharp angles composing the current biasing wires acts as mirrors for high frequency components of the control parameters. (b) Circuital representation of the device. Two currents (I_S and I_D) flow in two sections of the superconducting loops, while the device is entirely pierced by a uniform magnetic field (B). (c) and (d) Stability diagrams measured at $T = 30$ mT showing the differential conductance $dI_{\mathrm{SD}}/dV_{\mathrm{SD}}$ at different n_G and V_{SD} values when $\Phi_S = \Phi_D = 0$ (c) and $\Phi_S = \Phi_D = \Phi_0/2$ (d). Here, the magnetic fluxes are induced by the external magnetic field B. Black arrows indicating $2V_1$ and $2V_2$ represent the voltage region where the current is blocked by either the superconducting gaps of the island and the electrodes or the charging energy.

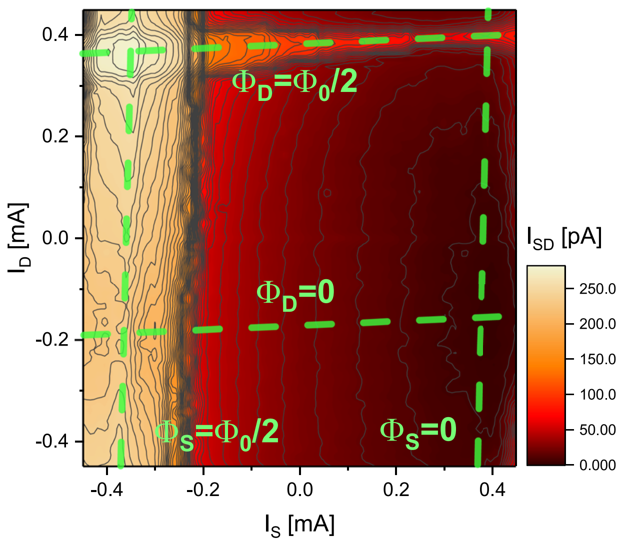

FIG. 2. Contour plot of the source–drain current at fixed bias voltage ($V_{SD} = V_1$) vs on-chip control currents (I_S and I_D). $B = 0.0875$ mT is applied leading to the condition $\Phi_B = \Phi_0/4$, and the device temperature is set to be $T = 700$ mK.

peaks (JQPs).[14,22–25] In particular, dark and sharp JQP conductance peaks clearly visible in the blocked region of Figs. 1(c) and 1(d) are unaffected by the small magnetic field applied since they depend on the island superconducting gap Δ_I and E_C only. Therefore, from the JQPs, we have estimated $\Delta_I \approx 216$ μeV. When the SQUISET is uniformly pierced by B, the condition $\Phi_S = \Phi_D = \Phi_B = \Phi_0/2$ can be reached, as shown in Fig. 1(d), and the superconducting gaps of the two nanowires are reduced to their minimum via quantum interference. This effect can be appreciated by the reduction of the voltage threshold separating the conducting region, where the transport is dominated by quasiparticle tunneling and not JQP cycles, with respect to the blocked one [$V_1 = 2\Delta_I + \Delta_{S,0} + \Delta_{D,0}$ in Figs. 1(c) and $V_2 = 2\Delta_I + \Delta_{S,1/2} + \Delta_{D,1/2}$ in Fig. 1(d)]. It is worth mentioning here that V_1 and V_2 have been selected as reference thresholds, for which the independence by the charging energy E_C is guaranteed by their position with respect to the Coulomb diamonds. From there, the zero magnetic field and the $\Phi_0/2$ superconducting gaps of the electrodes have been deduced ($\Delta_{S,0} = \Delta_{D,0} \approx 235$ μeV and $\Delta_{S,1/2} = \Delta_{D,1/2} \approx 84$ μeV). The effect of local magnetic flux biasing via I_S and I_D is shown in Fig. 2, where the source–drain current I_{SD} is monitored at fixed bias $V_{SD} = V_1$ as a function of the currents flowing in the loops. The non-symmetrical behavior shown in Fig. 2 suggests an asymmetry in the dynamical conductance of the two tunnel junctions involved. From the analysis of maxima and minima fitted positions in this diagram, represented by quasi-orthogonal light green dashed lines, it is possible to observe and quantify the effect of the self-inductances, giving $M_S = 0.69\Phi_0/\text{mA}$ and $M_D = 0.87\Phi_0/\text{mA}$. From these estimates, the cross-influence of the flux control lines turns out to be almost negligible ($m_{S,D} < 0.05\Phi_0/\text{mA}$) and the electrode quasiparticle density of states are almost independently tunable by I_S and I_D, respectively. In order to further investigate the effect of an independent flux biasing via local effects, we have performed temperature series measurements that confirm the single charge sensitivity of our device up to $T = 700$ mK [Fig. 3(a)]. There, a symmetrical magnetic flux biasing condition via B respects the periodical modulation of the source–drain current when the device is biased at $V_{SD} = V_1$. It is worth mentioning that experimental data reported in Fig. 3 are affected by unavoidable background charge as commonly occurs in single charge sensitive devices. These offsets were removed by referring to the n_G normalized quantized induced charge value, whose zero is centered in one of the I_{SD} minima. By exploiting this evidence, we proceeded investigating the effect of local magnetic and electrical gating at $T = 700$ mK and two

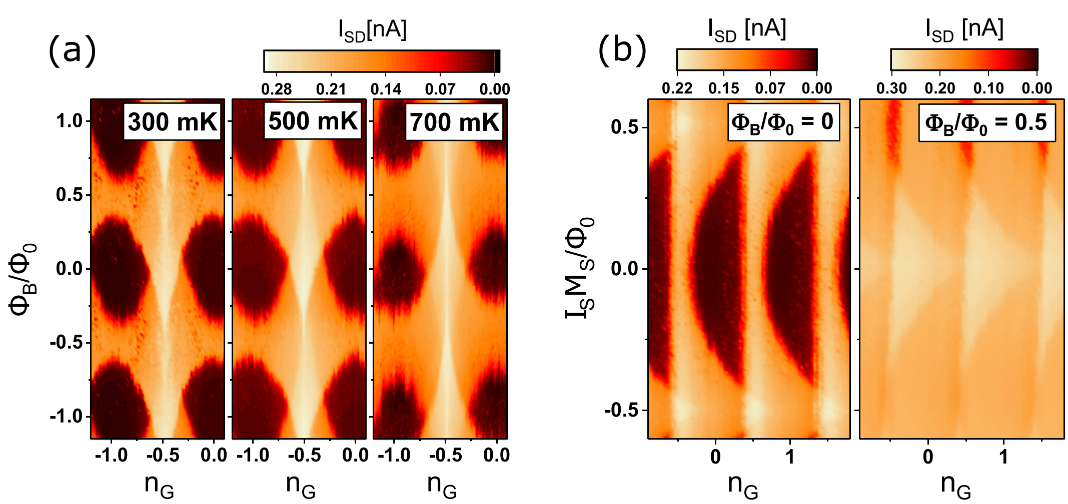

FIG. 3. (a) Source–drain current (I_{SD}) vs normalized gate voltage (n_G) and magnetic flux (Φ_B) at different bath temperatures. (b) Source–drain current in magnetic flux (I_SM_S) and electrical n_G local gating condition at a fixed temperature ($T = 700$ mK) having superimposed a $\Phi_B = 0$ and $\Phi_B = \Phi_0/2$ magnetic flux offset. All the measurements were performed at the fixed bias condition $V_{SD} = V_1$.

different magnetic fields leading to $\Phi_B = 0$ and $\Phi_B = \Phi_0/2$ [see Fig. 3(b)]. There, the periodical and asymmetrical dependence of I_{SD} on n_G reflects the unbalanced condition of the electrode superconducting gaps that affects the conductance of the tunnel junctions, with clear similarities to the behavior reported in Fig. 3(a). Triangular regions in the n_G–I_S plane, corresponding to the maximum I_{SD} current, are shifted and expanded from the $I_S M_S = \Phi_0/2$ condition (when no external magnetic field is applied) to $I_S = 0$ when a uniform magnetic flux offset is introduced ($\Phi_B = \Phi_0/2$). Analogously, semi-circular regions corresponding to blockaded regions of almost zero I_{SD} current are shrunk and shifted around the $I_S M_S = \Phi_0/2$ condition. The mechanism of unbalanced response to the magnetic field is analyzed in detail in Fig. 4(a), where we report the evolution of the flux-modulated current (I_{SD}) at different I_S values. I_{SD} presents sharp and periodic peaks on top of broader peaks. The latter are controlled by I_S, which induces their gradual separation. Yet, the sharp structures depend only on I_D, while their sharpness stems from the asymmetry existing between local conductances of the source and drain tunnel junctions.[26] The S'ISIS" structure of our device expresses here strong asymmetrical behavior with respect to the symmetrical geometry, simply due to the local action of unbalancing flux given by self-inductance effects. Sharp peaks at $\Phi_B = \Phi_0/2$ are independent with respect to the current I_S and can be attributed to the island–drain junction, confirming the negligible correlation between the two flux control lines of our device. The wider plateau of I_{SD} can be shifted along the Φ_B axis at will by acting on the I_S current. These plateaus are clearly wider with respect to the sharp peaks of the island–drain junction due to the asymmetric voltage bias of the circuit [see Fig. 1(b)]. In order to quantify the flux-to-current transfer function, we show in Fig. 4(b) the numerical derivative of I_{SD} with respect to Φ_B. Double peaked transfer functions reflect the role of the two different superconducting gaps; moreover, the effect of the flux bias via I_S can be exploited to further increment the responsiveness of our device to the magnetic flux variation. As an example, when $I_S M_S = 0.22\Phi_0$, the two negative peaks collapse in one and effectively enhance the transfer function from $|dI_{SD}/d\Phi_B| \approx 1.6$ nA/Φ_0 to $|dI_{SD}/d\Phi_B| \approx 3.2$ nA/Φ_0. Eventually, non-negative responsiveness can be induced around $\Phi_B = 0$ when $0.22\Phi_0 < I_S M_S < 0.33\Phi_0$. The high responsiveness of the SQUISET to the magnetic field is a consequence of the Coulombic island enhancing the transfer function by acting as an energy filter[27] for the intermediate charge states involved in the transport processes. This flexible configuration confirms potential application of dynamical conductance-enhanced sensitivity to magnetic field variations in double-junction system embedding quantum interference based electrodes.

In summary, we have reported the fabrication and characterization of a fully superconducting SQUISET demonstrating local manipulation of charge and magnetic flux sensing via independent current and voltage control lines. We have discussed in detail the dependencies on the external magnetic field, gate voltage, flux bias currents, and temperature, which is possible due to the multiple-electrode design of the device. On one side, this proof-of-concept device opens up to an unprecedented tool to superconducting charge control, with quantum interference based nanostructured electrodes, to be used in quantum electronics[4] and metrology.[18,28,29] Moreover, straightforward integration with present quantum technologies[10] based on aluminum nanostructures is worth considering.

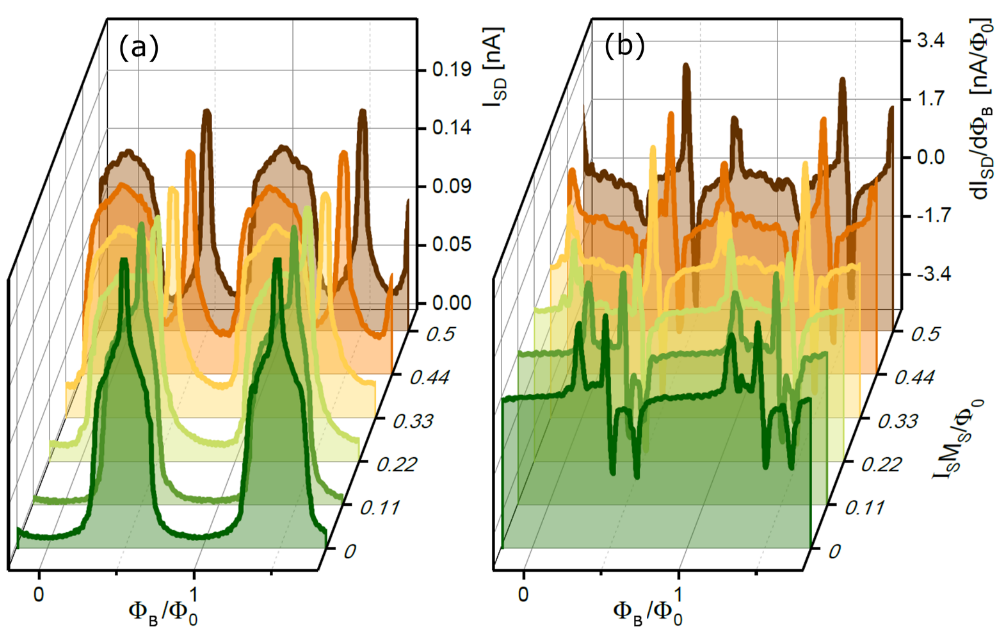

FIG. 4. (a) Flux-modulated current (I_{SD}) at different values of I_S. (b) Flux-to-current ($dI_{SD}/d\Phi_B$) transfer function obtained from numerical derivation of the curves in (a). All the measurements were performed at $n_G = 0$, $T = 700$ mK, and $V_{SD} = V_1$.

On the other side, the enhanced and flexible sensitivity to magnetic fields envisages our device concept for the implementation of energy-filtered[27] single charge magnetometers.

The authors gratefully acknowledge Compagnia di San Paolo for financial support to NanoFacility Piemonte at INRIM. They also thank G. Amato, L. Callegaro, and I. Mendes for helpful discussions. This work was supported by the INRiM "IBC-QuBit"—Seed Project. E.S. and F.G. acknowledge financial support from ERC Grant Agreement No. 615187—COMANCHE. F.G. acknowledges the Royal Society through the International Exchanges between the UK and Italy (Grant No. IESR3 170054). The work of F.G. was partially funded by the Tuscany Region under Grant No. FARFAS 2014 project SCIADRO.

AUTHOR DECLARATIONS

Conflict of Interest

The authors have no conflicts to disclose.

DATA AVAILABILITY

The data that support the findings of this study are available from the corresponding author upon reasonable request.

REFERENCES

[1] F. Giazotto, J. T. Peltonen, M. Meschke, and J. P. Pekola, "Superconducting quantum interference proximity transistor," Nat. Phys. **6**, 254 (2010).
[2] A. Ronzani, S. D'Ambrosio, P. Virtanen, F. Giazotto, and C. Altimiras, "Phase-driven collapse of the Cooper condensate in a nanosized superconductor," Phys. Rev. B **96**, 214517 (2017).
[3] S. D'Ambrosio, M. Meissner, C. Blanc, A. Ronzani, and F. Giazotto, "Normal metal tunnel junction-based superconducting quantum interference proximity transistor," Appl. Phys. Lett. **107**, 113110 (2015).
[4] V. Uri and D. Michel, "Introduction to quantum electromagnetic circuits," Int. J. Circuit Theory Appl. **45**, 897–934 (2017).
[5] E. Strambini, S. D'Ambrosio, F. Vischi, F. S. Bergeret, Y. V. Nazarov, and F. Giazotto, "The ω-SQUIPT as a tool to phase-engineer Josephson topological materials," Nat. Nanotechnol. **11**, 1055 (2016).
[6] P. Virtanen, A. Ronzani, and F. Giazotto, "Spectral characteristics of a fully superconducting SQUIPT," Phys. Rev. Appl. **6**, 054002 (2016).
[7] E. Enrico and F. Giazotto, "Superconducting quantum interference single-electron transistor," Phys. Rev. Appl. **5**, 064020 (2016).
[8] E. Enrico, E. Strambini, and F. Giazotto, "Phase-driven charge manipulation in hybrid single-electron transistor," Sci. Rep. **7**, 13492 (2017).
[9] T. A. Fulton and G. J. Dolan, "Observation of single-electron charging effects in small tunnel junctions," Phys. Rev. Lett. **59**, 109–112 (1987).
[10] J. Clarke and F. K. Wilhelm, "Superconducting quantum bits," Nature **453**, 1031 (2008).
[11] X. Gu, A. F. Kockum, A. Miranowicz, Y.-x. Liu, and F. Nori, "Microwave photonics with superconducting quantum circuits," Phys. Rep. **718-719**, 1–102 (2017), special issue on microwave photonics with superconducting quantum circuits.
[12] H. Pothier, P. Lafarge, C. Urbina, D. Esteve, and M. H. Devoret, "Single-electron pump based on charging effects," EPL (Europhys. Lett.) **17**, 249 (1992).
[13] J. P. Pekola, J. J. Vartiainen, M. Möttönen, O.-P. Saira, M. Meschke, and D. V. Averin, "Hybrid single-electron transistor as a source of quantized electric current," Nat. Phys. **4**, 120 (2007).
[14] D. V. Averin and Y. V. Nazarov, "Single-electron charging of a superconducting island," Phys. Rev. Lett. **69**, 1993–1996 (1992).
[15] Y. Nakamura, Y. A. Pashkin, and J. S. Tsai, "Coherent control of macroscopic quantum states in a single-Cooper-pair box," Nature **398**, 786 (1999).
[16] J. M. Martinis, M. Nahum, and H. D. Jensen, "Metrological accuracy of the electron pump," Phys. Rev. Lett. **72**, 904–907 (1994).
[17] S. d'Hollosy, M. Jung, A. Baumgartner, V. A. Guzenko, M. H. Madsen, J. Nygård, and C. Schönenberger, "Gigahertz quantized charge pumping in bottom-gate-defined inas nanowire quantum dots," Nano Lett. **15**, 4585–4590 (2015).
[18] S. P. Giblin, M. Kataoka, J. D. Fletcher, P. See, T. J. B. M. Janssen, J. P. Griffiths, G. A. C. Jones, I. Farrer, and D. A. Ritchie, "Towards a quantum representation of the ampere using single electron pumps," Nat. Commun. **3**, 930 (2012).
[19] A. J. Manninen, R. S. Poikolainen, T. V. Ryynänen, and J. P. Pekola, "Proximity-induced Josephson-quasiparticle process in a single-electron transistor," Phys. Rev. B **59**, R14161–R14164 (1999).
[20] N. Ligato, G. Marchegiani, P. Virtanen, E. Strambini, and F. Giazotto, "High operating temperature in V-based superconducting quantum interference proximity transistors," Sci. Rep. **7**, 8810 (2017).
[21] Y. Nakamura, T. Sakamoto, and J.-S. Tsai, "Study of Josephson-quasiparticle cycles in superconducting single-electron transistors," Jpn. J. Appl. Phys. **34**, 4562 (1995).
[22] Y. Nakamura, C. D. Chen, and J. S. Tsai, "Quantitative analysis of Josephson-quasiparticle current in superconducting single-electron transistors," Phys. Rev. B **53**, 8234–8237 (1996).
[23] A. N. Korotkov, "Charge sensitivity of superconducting single-electron transistor," Appl. Phys. Lett. **69**, 2593–2595 (1996).
[24] T. A. Fulton, P. L. Gammel, D. J. Bishop, L. N. Dunkleberger, and G. J. Dolan, "Observation of combined Josephson and charging effects in small tunnel junction circuits," Phys. Rev. Lett. **63**, 1307–1310 (1989).
[25] A. M. van den Brink, G. Schön, and L. J. Geerligs, "Combined single-electron and coherent-Cooper-pair tunneling in voltage-biased Josephson junctions," Phys. Rev. Lett. **67**, 3030–3033 (1991).
[26] L. Fasolo, D. Borchia, and E. Enrico, "Magnetic flux sensing exploiting two SQUIPTs connected by means of a floating island," IEEE Trans. Appl. Supercond. **31**, 3059983 (2021).
[27] P. Bhadrachalam, R. Subramanian, V. Ray, L.-C. Ma, W. Wang, J. Kim, K. Cho, and S. J. Koh, "Energy-filtered cold electron transport at room temperature," Nat. Commun. **5**, 4745 (2014).
[28] J. P. Pekola, O.-P. Saira, V. F. Maisi, A. Kemppinen, M. Möttönen, Y. A. Pashkin, and D. V. Averin, "Single-electron current sources: Toward a refined definition of the ampere," Rev. Mod. Phys. **85**, 1421–1472 (2013).
[29] N.-H. Kaneko, S. Nakamura, and Y. Okazaki, "A review of the quantum current standard," Meas. Sci. Technol. **27**, 032001 (2016).